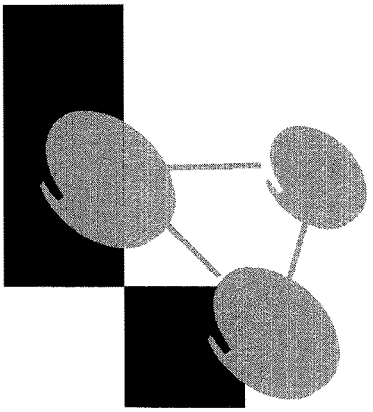

Virtual Reality (1999) 4:203-212

Banded Matrix Approach to Finite Element Modelling for Soft Tissue Simulation

J. Berkley[1], S. Weghorst[1], H. Gladstone[2], G. Raugi[2], D. Berg[2], M. Ganter[3],

[1]Human Interface Technology Lab; [2]Division of Dermatology; [3]Department of Mechanical Engineering, University of Washington, Seattle, WA, USA

Abstract: Realistic deformation of computer-simulated anatomical structures is computationally intensive. As a result, simple methodologies not based in continuum mechanics have been employed for achieving real-time deformation of virtual anatomy. Since the graphical interpolations and simple spring models commonly used in these simulations are not based on the biomechanical properties of tissue structures, these "quick and dirty" methods typically do not represent accurately the complex deformations and force-feedback interactions that can take place during surgery. Finite Element (FE) analysis is widely regarded as the most appropriate alternative to these methods. Extensive research has been directed toward applying this method to modelling a wide range of biological structures, and a few simple FE models have been incorporated into surgical simulations. However, because of the highly computational nature of the FE method, its direct application to real-time force-feedback and visualisation of tissue deformation has not been practical for most simulations. This limitation is due primarily to the overabundance of information provided by the standard FE approaches. If the mathematics are optimised through preprocessing to yield only the information essential to the simulation task, run-time computation requirements can be reduced drastically. We are currently developing such methodologies, and have created computer demonstrations that support real-time interaction with soft tissue. To illustrate the efficacy and utility of these fast "banded matrix" FE methods, we present results from a skin suturing simulator which we are developing on a PC-based platform.

Keywords: Virtual reality; Surgical simulation; Real-time analysis; Finite element modelling; Haptic feedback; Soft tissue

Introduction

Computer graphics reconstruction of complex human anatomy has provided excellent tools for anatomical visualisation (for numerous examples of anatomy reconstructions, see the Visible Human web site at www.nlm.gov). However, developing realistic virtual reality surgical simulation environments has proven a difficult challenge, and real-time interaction with such reconstructions has yet to realise its full potential. When tissue deformation is required, computation time can become a severely limiting factor. To achieve real-time interaction, "quick and dirty" methodologies are often incorporated, such as non-uniform rational B-spline (NURBS), bezier patch, and other methods based on polynomial interpolation [1,2,3,4]. With these approaches, deformation is dependent on the displacement of local control points. Physical relationships such as mass, inertia, applied force, etc., do not come into play in such calculations.

Haptic interaction, or force-feedback, is an essential component for many soft tissue simulation purposes, but also significantly increases the demand for computational power. Smooth force-feedback requires an update rate of 300-1000 Hz [5]. Like many of the ad hoc methods for simulating tissue deformation, force interactions are often calculated without regard to continuum mechanics. In some applications, only the depth at which a tool penetrates the tissue surface determines the reaction force [1,4,6,7]. More complex spring models have been utilised that incorporate matrices built from linear [8,9,10]; however, spring models are limited in that one-dimensional elements cannot always be connected in a fashion to achieve three-dimensional continuum mechanics.

FE analysis is a highly regarded alternative for modelling tissue deformation. While the acquisition of soft tissue material properties is not a simple matter, the methodologies do exist [11,12]. Soft tissue material properties are easily inserted into FE models in order to yield accurate continuum mechanic based models. Considerable work has been directed toward applying such models to the study of biological structures, including skin, fat, muscle, cartilage, bone, heart and brain tissue [13, 14,15,16,17,18]. However, because of the highly computational nature of the FE method, its direct application to providing force-feedback and real-time visualisation of tissue deformation is not practical in most cases.

There are few examples of the application of FE analysis to real-time simulation. To address this objective, we have developed the "banded matrix" technique (described in below) as a means for achieving real-time deformation and force feedback.This method is applicable to a wide range of soft tissue simulations. Our initial efforts have been dedicated to the development of a skin suturing simulator.

Finite Element Methods

In FE analysis, the governing matrix equation is

$$Md''+Dd'+Kd=f$$

where M is the mass matrix, D is the damping matrix, K is the stiffness matrix, d is the nodal displacement and f is the applied force. The size of each matrix is $n \times n$, where n is the number of nodes in the model times the degrees of freedom (three, in the case of three-dimensional effects). In static analysis, mass and damping components are set to zero. Each of these matrices is assembled from the elements of a FE mesh. Since the elements are of simple shapes (e.g. tetrahedrons), continuum mechanics can be used to define their behaviour. By assembling these elements together, the behaviour of a material with rather complex geometry can be approximated. The accuracy of an FE model increases with the number of elements used to approximate its geometry.

Some simulations simply use FE analysis for its predictive value, and do not require real-time computation. Both Larabee [19] and Pieper et al. [20] have used the FE method to predict the results of certain plastic surgeries. Animation of muscle contraction and skin deformation during grasping have been based on the FE [21,22]. Some investigators have simply used FE analysis to optimise simulators that utilise alternative methods for providing force-feedback and deformation [23].

An intriguing incorporation of FE analysis in real-time deformation has been presented by Cotin et al. [24]. Deformation of each node is controlled by a series of tensors that have been optimised based on FE deformation results. A single contact node is initially deformed in the x, y, and z directions and the resulting displacements of every other node are recorded. A tensor is developed through optimisation techniques that will transform the displacement of the contact node into the displacement of a remote node. Each node is associated with multiple tensors to account for every possibility of nodal contact. While this methodology does not give exact FE solutions, it does provide a means for approximating FE results for high-order models.

Small FE models (models with a small number of nodes) have been incorporated into surgery simulators. Simultaneous evaluation of algebraic equations is achieved through matrix operations. In linear analysis, an $n \times n$ stiffness matrix (where n is the *total* number of nodes times the degrees of freedom) is assembled, inverted and multiplied by the applied forces to obtain displacements. This is the "classical" method for solving static FE equations. Classical analysis may also include additional matrix oppressions for determining element stresses and strains. Stiffness matrix assembly, inversion and multiplication are expensive computationally, which limits the size of a model that can be solved in real-time.

Computational demands substantially increase with dynamic analysis, non-linear analysis and situations where the mesh is actively changing (i.e. cutting). The virtual environment for eye surgery

that was proposed by Sagar et al. [25] is therefore especially noteworthy. Cornea deformation is based on a nonlinear elastic material (Mooney-Rivilin material), and cutting is allowed. This was also one of the first applications to use distributed parallel processing to separate graphical rendering from mathematical computation in order to increase performance speed. The model contained only a small number of elements, but NURBS (Non-Uniform Rational B-Splines) were used to interpolate among nodes. This gave the appearance of a much higher-order model. However, the simulation did not provide real-time computation in that the results of the deformation were presented only once per second.

Classical FE analysis yields an overabundance of information and is time intensive. In surgery simulation, we are usually only concerned with the displacement of surface nodes (or the nodes we can see), and the reaction force at the point of contact. If the mathematics are optimised in a preprocessing stage to yield only the necessary information, computation time can be drastically reduced. Bro-Nielsen and Cotin [26] have applied such strategies to achieve real-time deformation. They apply a process known as condensation to reduce the problem from a size of $n \times n$ to the size of $v \times v$ (where v is the number of *visible* nodes times the degrees of freedom). This reduction in matrix size reduces the time needed for processing the matrix. The reduced stiffness matrix is inverted to permit the calculation of visible nodal displacements. Real-time calculation is dependent only on how quickly the inverted condensed stiffness matrix can be multiplied by the applied forces. This reduced format gives eactly the same results as can be obtained with classical FE solution methodologies. Using a Silicon Graphics ONYX with four MIPS R4400 processors, a model of the lower leg with 250 visible nodes was deformed with a visual update of 20 Hz. In this demonstration, a numerical force was applied to one node, and force feedback to the user was not incorporated.

Banded Matrix Algorithm

FE modelling for surgical training simulation does not require the detailed results that are obtained with typical computer aided design (CAD) packages. In general, only the displacements of surface nodes and the force resulting from surgical instrument contact are required in these simulations. Because interior nodes cannot be seen, there is no reason to calculate their displacements. Rearrangement of the FE equations can prioritise calculation and insure that results at the surface of the model will be solved first (Fig. 1a). Rows and columns are swapped so that the first set of rows and columns correspond to *boundary condition nodes*. The *interior nodes* correspond to the nodes where displacements do

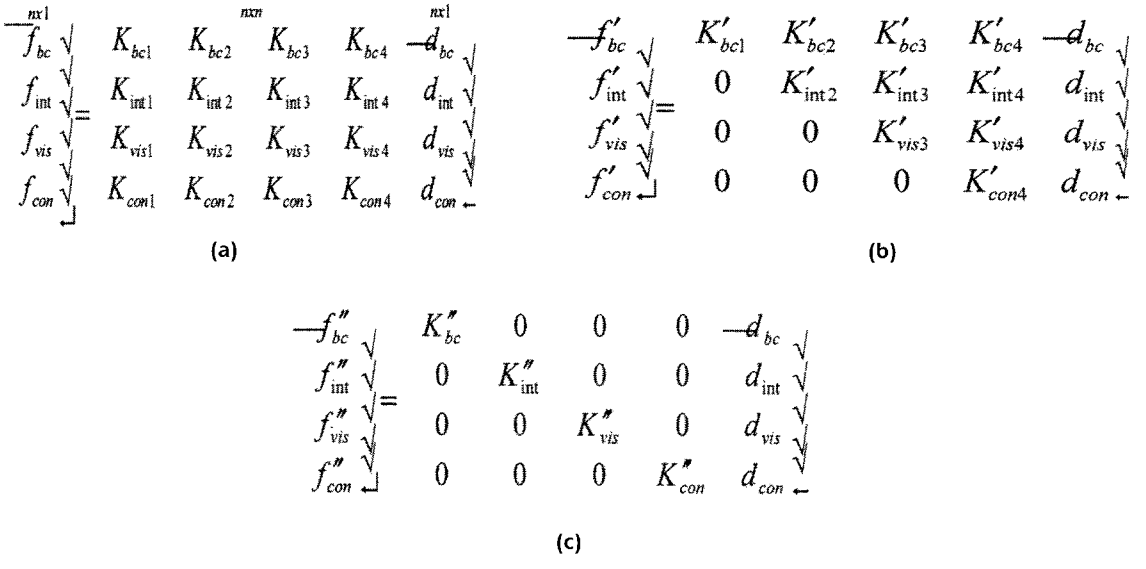

Fig. 1. The steps for optimising FE equations, where bc = boundary condition nodes, int = interior nodes, vis = nodes included in visible elements, and con=contact nodes. K_{type-j}, d_{type} and f_{type} represent different subsections of the stiffness matrix, displacement vector and force vector respectively. Apostrophes indicate a new permutation of a matrix structure.

not need to be calculated. These are usually nodes in the interior of the model that cannot be seen and are not needed for surface element stress-strain calculations. The next set of nodes, the *visible nodes*, consists of the nodes contained in the elements lying on the surface of the model. These nodes are given priority since they must be accounted for when calculating and rendering the displacement, stress and strain at the geometry surface.

In most cases, the user needs to touch only what he or she can see. This gives a set of contact possibilities that is directly related to the number of element faces that lie on the surface of the model. The stiffness matrix can be arranged to optimise calculation speed for each of the element faces that might be contacted by the user's instrument. Given a single point of displacement on an element face, the displacement can be distributed among the nodes of the face using shape functions. These nodes are considered to be the *contact nodes*. For each set of contact nodes, the stiffness matrix is arranged so that the rows and columns corresponding to the contact nodes are pivoted to the bottom rows and the columns farthest to the right. The displacement and force vectors are likewise pivoted. Gaussian elimination is then applied down to the contact nodes to achieve an upper triangulated matrix (Fig. 1b). This decouples visible and contact node displacement calculations from interior and boundary condition variables. Interior and boundary nodes still contribute to the overall behaviour of the model; however, their contributions have been "dumped" into K'_{vis}, K'_{con}, f'_{vis} and f'_{con}.

Upper triangulation of the stiffness matrix takes place in the preprocessing stage. Additional matrix refinement can also be applied at this time. Backward Gaussian elimination can be used to "band" the matrix (Fig. 1c). The end result is a matrix filled with zeros, except for a diagonal band with a width equal to three times the number of contact nodes, plus one. The reason for the "plus one" is that during Gaussian elimination, only equations with known applied forces can be used in equation addition and subtraction. During the pre-processing stage, the applied forces at the contact nodes are not known. Therefore, backward Gaussian elimination must begin with the last equation that represents a visible node with a known applied force. This force is usually equal to zero, unless specific boundary conditions have been applied. After banding is complete, the zeros are discarded and only the band is stored. Each set of contact nodes has a specific banded matrix, and all of these matrices must be stored in anticipation of any possible contact scenario.

The bottom portion of the banded matrix (Fig. 1c) is used to calculate reaction forces given a set of contact node displacements. The equation for calculating force-feedback at the contact nodes is $f_{con} = K_{con}\, d_{con}$. K_{con} is a $p \times p$ matrix where p is three times the number of contact nodes. If a single point of displacement is distributed over three nodes of a tetrahedral element face, K_{con} is only a 9 x 9 matrix. Shape functions are used to find the reaction force at the point of contact given the forces resulting at the contact nodes. It is this force that is sent to the force-feedback device. Force-feedback is effectively decoupled from the rest of the surface node displacement calculations. Such a small matrix allows for a haptic update rate well over 1000 Hz, which is considered optimal for providing smooth force-feedback.

Given a set of reaction forces and displacements at the contact nodes, backward substitution can be used to obtain the remaining surface node displacements, which are used for the graphical display of deformation. The displacements are calculated in a thread separate from the haptic update calculations. In our PC-based suturing simulator described below, these calculations are performed at 30 Hz, a rate adequate for smooth real-time graphical rendering. Additional information, such as surface stress and strain, can also be calculated at this time.

Typically the only force applied to the model results from contact with the user's tool. Everywhere else the applied force is zero. Calculations are simplified, since $f_{bc}=f_{int}=f_{vis}=0$. The force vector does not need to be reduced during Gaussian elimination and can be ignored.

It is possible, however, to apply constant forces other than those applied by the tool. For example, to simulate the pre-tension that exists in skin, a constant tension may be applied to a defined set of nodes If additional constant forces are applied, it is necessary to reduce the force vector while reducing the stiffness matrix, as normally takes place in Gaussian elimination. Thus, each banded matrix will be associated with a unique force vector.

In the case of multiple point contact, such as when using multiple tools, the principle of superposition is used to determine deformation. The principle of suppression insures that the resulting deformation from all point loads applied will be the same, independent of the order in which these loads have been applied. The contributing deformation resulting from each point of contact is found by using the appropriate banded matrix. All deformation contributions are summed together to determine the overall deformation.

Banded Matrix Algorithm Performance

When using banded matrices, the processing time during simulation increases linearly with an increase in the number of surface nodes or an increase in the number of nodes displaced. An increase in the number of interior nodes or boundary condition nodes does not affect simulation performance. This is in contrast to classical FE analysis where the number of calculations required increases exponentially with an increase in the number of nodes.

Model size is limited by the manner in which the banded matrices are stored. In our current applications, banded matrices are not loaded from storage into RAM until contact is made. When taking this approach, model size is thus limited by how quickly a banded matrix can be loaded. Using a low-end PC and a SCSI 4 card, which can access storage at 80 Mbytes per second, a model with 30,303 surface nodes can be loaded in a tenth of a second. With bigger models the delay caused by loading a banded matrix becomes perceptible. If enough RAM is available ($264*v^2$ bytes where v is the number of visible nodes), all the banded matrices can be loaded when the simulation begins. Note that with these banded matrix FE techniques, the time needed to calculate deformation and force-feedback is insignificant when compared to the time needed for graphical rendering.

In terms of calculation time requirements, the banded matrix technique is vastly superior when compared to the conventional application of FE equations. To illustrate the difference in calculation time, a comparison is provided Consider a 3D fast finite element model with 1000 total nodes (n=1000), 600 of which are visible (v=600), with a set of constant applied forces, and a single point of applied displacement distributed over three nodes (p=3). A total of $3v(6p-1) + 3p(6p-1) =$ (displacement calculations) + (force calculations) = 30,753 computations are required during run-time to obtain force-feedback and deformation. With a standard FEM approach, the necessary computations vary depending on how the equations are solved. A total of

$$1/3(3n)^3 + 1/2(3n)^2 + 1/2(3v)^2 = 9.006 \times 10^9$$

calculations are required when LU decomposition is used to find the displacement of the visible nodes (sparcity of the matrix not taken into account). It might be argued that this number could be drastically reduced if only forces, rather than displacements, are applied at contact nodes. With this approach all of the unknown variables would lie in the displacement vector. The displacements could then be effectively solved by inverting the stiffness matrix in the pre-processing stage and multiplying it by the force vector at run-time. Under these conditions, only $3v(6n-1) = 10,798,200$ calculations are required to obtain deformation while the simulation is running. Matrix inversion is still undesirable, since it requires 351 times as many computations as the banded matrix technique. This performance advantage increases exponentially as the number of nodes increases.

In addition, it should be noted that most force-feedback devices (e.g. the *PHANTOM™* from SensAble Technologies, Incorporated) *yield* end-effector displacements and *require* an input force. Therefore, the direct application of forces to contact nodes is not always practical.

Clinical Application

A single approach is not sufficient for all situations. A simulation's specific emphasis may be on deformation visualisation, haptic interaction at one or multiple points, stress development within the

Table1. Taxonomy of relevant soft tissue task scenarios.

Scenario	Mesh type	Surgical tool modelling	Example
1*	Static mesh (mesh not changing, i.e. no cutting)	Rigid	Dermatological excision closure; Orthoscopic palpation
2	Dynamically changing mesh (allows for cutting)	Rigid	Endoscopic dissection; Open procedures
3, 4	Static and dynamic meshes	Deformable	Catheterisation procedures

* Achieved with banded matrices

tissue, alteration of tissue structures (i.e. cutting or dissection), or all of the above. The banded matrix technique is appropriate only when the FE mesh is unchanging, such as when closing an excision or navigation during endoscopy.

Table 1 describes various modelling scenarios that encompass the majority of surgical tasks. While the overall goal of our research programme is to develop appropriate methodologies for optimising FE equations for each of these surgical simulation scenarios, we focus here on Scenario 1.

Skin Suturing Simulation

The ability to perform skin surgery at its most basic level, that of making simple incisions and basic suturing, is a necessary skill for medical students planning to practise in primary care [27]. It is also an important skill for those training in the allied health care fields. Most students learn the rudiments of skin surgery in the emergency room by suturing various traumatic wounds, in the obstetrical suite by suturing episiotomy incisions or lacerations, or in didactic sessions using pigs' feet.

Several limitations are imposed by these teaching methods: (1) The nature of the physician–patient interaction mitigates against honing surgical skills in clinical settings by both ethical and time constraints; (2) pigs' feet provide a poor simulation of the range of biomechanical properties of human skin, do not compare well with human anatomy, and raise potential religious conflicts with the use of porcine tissues among certain Jewish and Islamic students and practitioners; and (3) training on live cases introduces risk of exposure to blood-borne pathogens in students and trainees, who may be least adept with surgical sharp instruments.

We anticipate that training experience on such a simulator will increase the students' confidence in performing simple excisions and closures, will increase their technical proficiency [28], and will decrease the time required to complete these procedures, as well as reduce the likelihood of self injury.

We have begun the development of a skin suturing simulator that allows for incision closure. The simulator is based on Microsoft Foundation Classes and is currently being run on a single-processor PC with a 300-MHz Pentium II processor. Separate computational threads run the graphical and haptic update calculations. Force-feedback is accomplished via a *PHANTOM Premium* device from SensAble Technologies, Inc., which can produce forces ranging from 0 to 8.5 Newtons. This range is more than adequate for simulating the forces

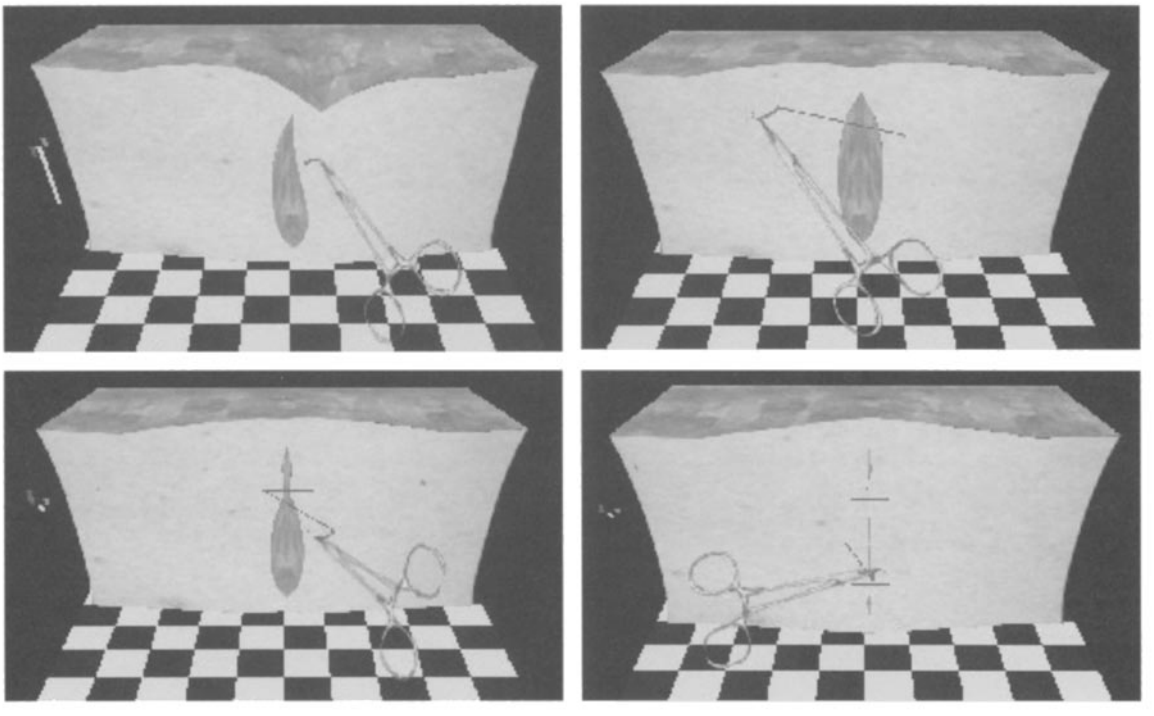

Fig. 2. Screen captures of skin suturing simulator based on the banded matrix technique.

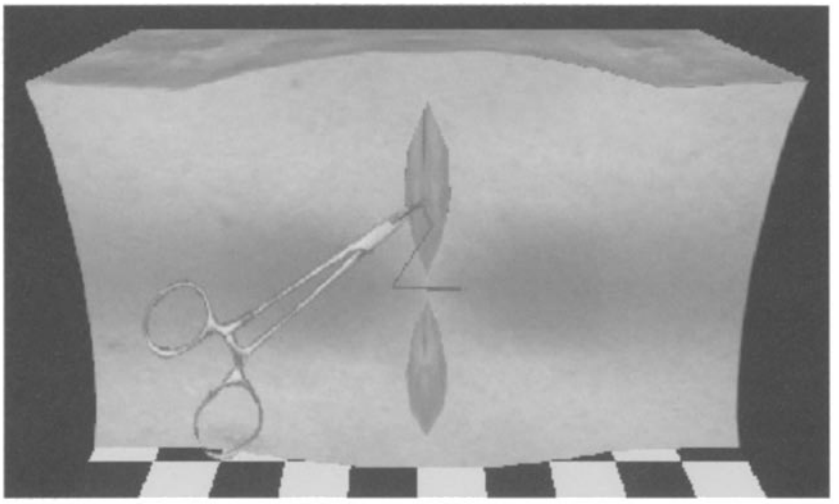

Fig. 3. Colour overlay of stress magnitudes can be used to provide feedback and to assess the user's suturing technique.

required during suturing. The user controls the *PHANTOM* by grasping a needle holder, which has been attached to the end of the *PHANTOM* arm. The movement of the needle holder is mirrored by a virtual needle holder on the computer screen.

The simulator presents a pre-incised wound that can be closed through suturing (Fig. 2). As a training aid, the simulator includes an option that allows colour overlay plots that represent tissue strains and stresses. This helps in identifying improper techniques that might lead to tissue damage and necrosis (Fig. 3).

Effort is currently being directed toward creating a software package that allows fast FE models to be created from medical images. Using contours extracted from MRI or CT scans, implicit models of anatomical structures can be generated. Using the "point repulsion" method [29], nodes are evenly distributed throughout the volume of the model. Standard tetrahedral meshing algorithms are then employed to create a finite element mesh, with material properties distributed based on scan pixel intensities [30]. If desired, the mesh can be altered to yield wounds or tissue defects. The final FE model is then converted to a fast FE model. This procedure allows for models of a variety of anatomical sites to be quickly generated. Figure 4 shows an example of a fast FE virtual arm model based on point repulsion node generation from a CAD-based implicit model.

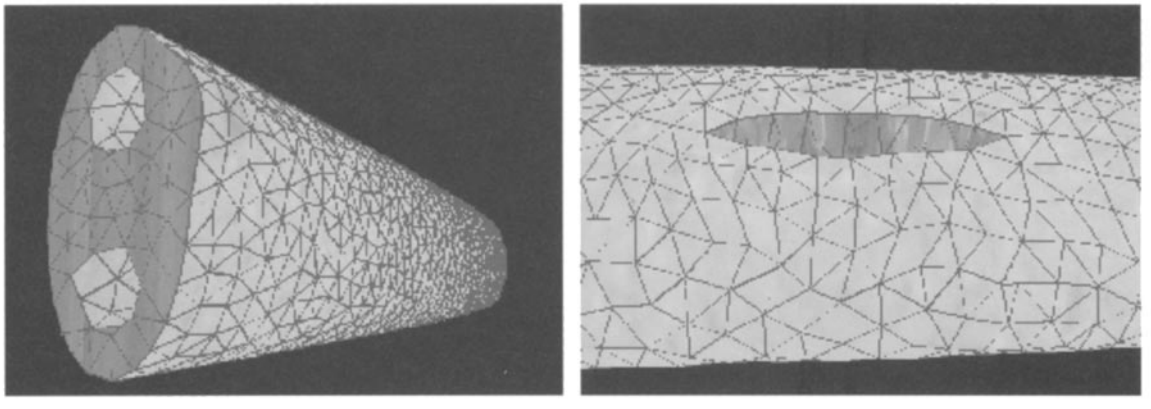

Fig. 4a. Fast FE model of a simulated arm created from an artistically created implicit solid model; **b.** Arm model with an incision.

Discussion

The main advantage of the banded matrix technique is its substantially reduced run-time computation requirements, which enable realistic real-time tissue interaction. The main limitation of the technique is that the original mesh cannot be changed while the simulation is running. All preprocessing is based on the original mesh. If it is necessary to make a change to the original model, such as during cutting, then all of the pre-processing must be repeated to determine a new set of banded matrices and force vectors. If a cut will be made along a defined path, it is possible to create appropriate banded matrix models in anticipation of different phases of the cut. However, this approach is limited by storage requirements since a vast array of banded matrix models must be created in order to anticipate all of the possible cutting scenarios. While outside the scope of the current report, several novel methods for achieving robust real-time cutting are under development and will be reported later.

An important point to consider is whether non-linear soft tissue can be represented with linear modelling. This raises the issue of how accurate a simulation needs to be. The specific objective of the simulator ultimately determines the answer to this question. If the goal is to create a realistic environment where the user becomes immersed in a surgical task, it is necessary to provide graphics and force-feedback that cannot be significantly distinguished from the real thing. If the goal is to improve a student's competency at a designated task, then the user's skill level must improve with use of the simulator, regardless of whether modelling inaccuracies are noticeable to the user.

Studies have yet to be performed to determine the requirements for haptic accuracy in typical suturing tasks. If a linear stress/strain curve is fitted to a non-linear curve, the resulting material properties may provide a user with haptic feedback that cannot be distinguished from force-feedback based on non-linear material properties. It stands to reason that at some point a user will be able to notice the difference between linear and non-linear force feedback; however, it is unknown exactly where this detectable error threshold lies. The detectable error threshold may be low if side-by-side comparison testing is conducted. However, the accuracy of a surgical simulator should not be judged by such criteria. Typically, the user must compare the accuracy of a simulator to his or her past experience. Under such circumstances, it is likely that a higher threshold would be reached before errors in force-feedback are noticeable. A simulator's value as a training tool degrades as these errors become more detectable. A similar argument could be made when comparing visual perception of linear and non-linear deformation.

The banded matrix technique described here uses linear material properties. The initial reaction from dermatological surgeons has been that the suturing simulator provides realistic force-feedback and deformation that is comparable to real skin. However, we are aware that material property testing of skin will not yield purely linear results. For this reason, we are investigating quasi-linear applications of the banded matrix method where a non-linear stress/strain curve is approximated by linear subsections. This method of representation has been proposed by Fung [11], where he describes various soft tissue stress/strain curves that consist of three separate linear phases.

The development of the skin excision closure simulator is still in its infant stage. While initial efforts provide proof of concept, many improvements must be made before the simulator can be used in a clinical setting. These include more accurate needle and thread modelling, better graphics, 3D visualisation through shutter glasses and/or a head mounted display, and the addition of computerised training aids and instructions. A thorough validation process is under way using methods emerging in the field of medical simulation [31], and transfer of simulation training to the clinical setting will be assessed.

Acknowledgements

This work was supported by the University of Washington Division of Dermatology, and by DARPA AASERT grant DAAH04-95-1-0471. Parts of this paper appeared in the proceedings of the *Medicine Meets Virtual Reality* conference [32].

References

1. Thingvold JA, Cohen E. Physical modelling with B-spline surfaces for interactive design and animation. Proc. Symposium on Interactive 3D Graphics 1990
2. Park J, Metaxas D, Jones A. Deformable models with parameter functions: application to heart-wall modelling. In: Proceedings of IEEE Computer Society Conference on Computer Vision and Pattern Recognition. IEEE Computer Society Press, 1994
3. Song G-J, Reddy NP. Tissue cutting in virtual environments. In: Interactive Technology and the New

Paradigm for Healthcare (Proceedings of Medicine Meets Virtual Reality). Morgan K, Satava RM, Sieburg HB, Mattheus R, Christensen JP, eds. Amsterdam: IOS Press, 1995; 359–364.

4. Hahn JK, Kaufman R, Winick AB, Carleton T, Park Y, Lindeman R, Oh K-M, Al-Ghreimil N, Walsh RJ, Loew M, Gerber J, Sankar S. Training environment for inferior vena caval filter placement. In: Medicine Meets Virtual Reality: Art, Science, Technology (Proceedings of Medicine Meets Virtual Reality). Westwood JD, Hoffman HM, Stredney D, Weghorst S. eds. Amsterdam: IOS Press, 1998; 291–297
5. Delingette H. Toward realistic soft-tissue modelling in medical simulation. Proceedings of the IEEE, 1998; 86(3): 512–523
6. Stredney D, Wiet G., Yagel R, Sessanna D, Kurzion Y, Fontana M, Shareef N, Levin M, Martin K, Okamura A. A comparative analysis of integrating visual representations with haptic display. In: Medicine Meets Virtual Reality: Art, Science, Technology (Proceedings of Medicine Meets Virtual Reality). Westwood JD, Hoffman HM, Stredney D, Weghorst S, eds. Amsterdam: IOS Press, 1998: 20–26
7. Tseng CS, Lee YY, Chan YP, Wu SS, Chiu AW. A PC-based surgical simulator for laparoscopic surgery. In: Medicine Meets Virtual Reality: Art, Science, Technology (Proceedings of Medicine Meets Virtual Reality). Westwood JD, Hoffman HM, Stredney D, Weghorst S. eds. Amsterdam: IOS Press, 1998: 155–160
8. Gibson S, Samosky J, Mor A, Fyock C, Grinson E, Kanade T, Kikinis R, Lauer H, MacKenzie N, Nakajima S, Ohkami H, Osborne R, Sawada A. Simulating arthroscopic knee surgery using volumetric object representations, real-time volume rendering and haptic feedback. Proceedings of the First Joint Conference CVRMed-MRCAS'97, Lecture Notes in Computer Science 1205: 369–378
9. Bro-Nielsen M, Helfrick M, Glass B, Zeng X, Connacher H. VR simulation of abdominal trauma surgery. In: Medicine Meets Virtual Reality: Art, Science, Technology (Proceedings of Medicine Meets Virtual Reality). Westwood JD, Hoffman HM, Stredney D, Weghors, S. eds. Amsterdam: IOS Press, 1998: 117–123.
10. Downes M, Cavusoglu MC, Gantert W, Way LW, Tendick F. Virtual environments for training critical skills in laparoscopic surgery. In: Medicine Meets Virtual Reality: Art, Science, Technology (Proceedings of Medicine Meets Virtual Reality). Westwood JD, Hoffman HM, Stredney D, Weghorst S. eds. Amsterdam: IOS Press 1998; 316–322
11. Fung YC. Biomechanics: mechanical properties of living tissues, 2nd ed. Berlin: Springer-Verlag, 1993
12. Hannaford B, Trujillo J, Sinanan M, Moreyra M, Rose, J, Brown J. Leuschke R, MacFarlane M. Computerized endoscopic surgical grasper. In: Medicine Meets Virtual Reality: Art, Science, Technology (Proceedings of Medicine Meets Virtual Reality). Westwood JD, Hoffman HM, Stredney D, Weghorst S. eds. Amsterdam: IOS Press, 1998: 258–264
13. Mow VC, Holmes MH, Lai WM. Fluid transport and mechanical properties of articular cartilage: a review. J Biomech 1984; 17: 377–394
14. Spilker RL, de Almeida ES, Donzelli PS. Finite element methods for the biomechanics of soft hydrated tissues: nonlinear analysis and adaptive control of meshes. Crit Rev Biomed Eng 1992; 20(3–4): 279–313
15. Ueno K, Melvin JW, Li L, Lighthall JW. Development of tissue level brain injury criteria by finite element analysis. J Neurotrauma 1995; 12(4): 695–706
16. Bradley CP, Pullan AJ, Hunter PJ. Geometric modelling of the human torso using cubic hermite elements. Ann Biomed Eng 1997; 25(1): 96–111
17. Keyak JH, Rossi SA, Jones KA, Skinner HB. Prediction of femoral fracture load using automated finite element modelling. J Biomech 1998; 31(2): 125–133
18. May-Newman K, McCulloch AD. Homogenization modelling for the mechanics of perfused myocardium. Prog Biophys Mol Biol 1998; 69(2–3): 463–481
19. Larrabee W. A finite element model of skin deformation: Biomechanics of skin and tissue: a review. Laryngoscope 1986; 96: 399–405
20. Pieper S, Rosen J, Zeltzer D. Interactive graphics for plastic surgery: a task-level analysis and implementation. Proc. Computer Graphics 1992; 25(2): 127–134
21. Gourret JP, Thalmann NH, Thalmann D. Simulation of object and human skin deformations in a grasping task. Proc. Computer Graphics (SIGGRAPH'89),1989; 23: 21–10.
22. Chen DT, Zeltzer, D. Pump it up: computer animation of biomechanically based model of muscle using the finite element method. Proc. Computer Graphics (SIGGRAPH'92), 1992; 26: 89–98
23. Keeve GB, Girod ES. Craniofacial surgery simulation. Proc. 4th Int. Conf. Visualization in Biomedical Computing (VBC'96), 1996; 541–546
24. Cotin S, Delingette H, Ayache, N. Real-time elastic deformations of soft tissue for surgery simulation. In-house publication. Institut National de Recherche en Informatique et en Automatique, 1998
25. Sagar MA, Bullivant D, Mellison GD, Hunter PJ, Hunter IW. A virtual environment and model of the eye for surgical simulation. Proc. ACM SIGGRAPH, 1994; 205–212
26. Bro-Nielsen M, Cotin S. Real-time volumetric deformable models for surgery simulation using finite elements and condensation. Computer Graphics Forum 1996; 15(3): 57–66
27. Thompson AM, Park KG, Kelly DR, MacNamara I, Munro A. Training for minor surgery in general practice: is it adequate? J Royal Coll Surg Edinb 1997; 42(2): 89–97
28. Sinclair MJ, Peifer JW, Halebian R, Luxenberg MN, Green K, Hull DS. Computer simulated eye surgery: a novel teaching method for residents and practitioners. Ophthalmology 1995; 102(3): 517–521
29. Brooking C. Point repulsion in implicit solids. In-house publication. Department of Mechanical Engineering, University of Washington, 1999; brooking@u.washington.edu
30. Berkley J. Determining soft tissue material properties for the purpose of Finite Element Modelling of the below knee smputee tesidual limb. Masters Thesis, Northwestern University, Chicago, IL, 1997
31. Weghorst S, Airola C, Oppenheimer P, Edmond CV, Patience T, Heskamp D, Miller J. Validation of the Madigan ESS simulator. In: Medicine Meets Virtual

Reality: Art, Science, Technology (Proceedings of Medicine Meets Virtual Reality). Westwood JD, Hoffman HM, Stredney D, Weghorst S. eds. Amsterdam: IOS Press, 1998; 399–405

32. Berkley J, Weghorst S, Gladstone H, Raugi G, Berg D, Ganter M. Fast Finite Element Modelling for surgical simulation. In: Medicine Meets Virtual Reality: The Convergence of Physical and Informational Technologies: Options for a New Era in Health Care (Proceedings of Medicine Meets Virtual Reality). Westwood JD, Hoffman HM, Robb RA, Stredney D. eds. Amsterdam: IOS Press, 1999; 55–61

Correspondence and offprint requests to:
Dr J Berkley, Human Interface Lab, Hayes Gladstone, University of Washington, Seattle, WA, USA. Email: weghorst@u.washington.edu